Available online at www.sciencedirect.com

ScienceDirect

Ceramics International 40 (2014) 1059–1063

CERAMICS INTERNATIONAL

www.elsevier.com/locate/ceramint

One-pot synthesis of grass-like Fe_3O_4 nanostructures by a novel microemulsion-assisted solvothermal method

Yanfen Li, Rongli Jiang*, Tingyu Liu, Hui Lv, Lu Zhou, Xiaoyu Zhang

School of Chemical Engineering and Technology, China University of Mining and Technology, Xuzhou 221116, PR China

Received 16 June 2013; received in revised form 26 June 2013; accepted 27 June 2013
Available online 4 July 2013

Abstract

Well-defined grass-like Fe_3O_4 nanostructures have been successfully synthesized via a novel and facile microemulsion-assisted solvothermal method. The resultant Fe_3O_4 products were characterized by X-ray diffraction (XRD), energy dispersive X-ray spectroscopy (EDX) and field emission scanning electron microscopy (FE-SEM). The effects of various reaction conditions on the morphology and structure of Fe_3O_4 products were investigated. The results show that the reaction temperature, the concentration of KOH and the reverse microemulsion system play important roles in governing the final product. The hysteresis loops of the grass-like Fe_3O_4 nanostructures were measured at room temperature, the superparamagnetic signature emerged with the saturated magnetization of 65.5 emu/g.
© 2013 Published by Elsevier Ltd and Techna Group S.r.l.

Keywords: C. Magnetic properties; Fe_3O_4; Grass-like nanostructures; Microemulsion-assisted solvothermal

1. Introduction

One-dimensional (1D) nanoscale materials have attracted tremendous attention in the area of nanotechnology because these materials exhibit unique morphology, optical, electronic, and magnetic properties which hold great promise for advanced catalysis, electronics, sensors, energy storage/conversion, and photonic applications [1–4].

During the past decade, considerable attention has been drawn to the preparation of magnetic micro/nanomaterials owing to their peculiar properties and technological applications [5,6]. Especially, as the oldest magnetic material and one of the most important magnetic materials, magnetite (Fe_3O_4) with advantages of low cost, non-toxicity, high chemical stability, good biocompatibility and natural abundance has aroused great interest due to their potential applications in a wide range of fields like lithium-ion batteries, biomaterials diagnostics, recoverable catalyst, ferrofluids, magnetic resonance imaging, immunoassay, water treatment, drug and gene delivery [7–10]. One-dimension Fe_3O_4 nanomaterials with anisotropic morphologies and perfect structures have outstanding physicochemical properties that are not conceivable in bulk structures [11–16]. Up to now, many efforts have been directed to the fabrication of Fe_3O_4 1D architectures. For example, Muraliganth et al. [17] prepared Fe_3O_4 nanowires by a microwave-hydrothermal approach. Yu et al. [18] synthesized Fe_3O_4 nano-whiskers via ultrasonic-aided reduction of $FeCl_2 \cdot 4H_2O$ with $N_2H_4 \cdot H_2O$ in concentrated NaOH solution. Zhang et al. [19] fabricated Fe_3O_4 nanorods through a reverse co-precipitation with external magnetic field-assisted strategy. Though much progress has been made in the synthesis of 1D magnetite micro/nanostructures, simple routes under milder conditions are still required.

As we all know, simple chemical reactions in reverse micelles or microemulsions have been shown to be powerful in controlling the size and shape of inorganic nanocrystals [20]. Reverse microemulsions are colloidal "nanodispersions" of water/oil stabilized by a surfactant and cosurfactant film [21,22]. Also, reverse microemulsions are thermodynamically stable systems and have the ability to solubilize proper solution. As the nanowater pools, they can provide ideal spatially constrained microreactors for the synthesis of inorganic nanoparticles with desired size and morphology. In addition, the solvothermal method has been widely applied to form nanomaterials for its unique reaction environment. It has been proven that the use of solvothermal method for generating nanomaterials cannot only

*Corresponding author. Tel.: +86 516 83885096; fax: +86 516 83591054.
E-mail address: ronglijcumt@163.com (R. Jiang).

0272-8842/$ - see front matter © 2013 Published by Elsevier Ltd and Techna Group S.r.l.
http://dx.doi.org/10.1016/j.ceramint.2013.06.104

decrease reaction temperature of systems but also improve the crystallinity of the products. Whereas the microemulsion-assisted solvothermal method, as a combination of the two methods mentioned above, possesses all the merits of both and has already been approved as an effectual tool to fabricate inorganic nanocrystals [23–25]. We also prepared In_2O_3 nanocubes [26] and ZnO nanotetrapods [27] by microemulsion-mediated solvothermal approach.

Herein, we further report the successful synthesis of grass-like Fe_3O_4 nanostructures by employing a nonionic TritonX-100-based reverse microemulsion system under solvothermal conditions. The effects of the reaction temperature, the concentration of KOH and the reverse microemulsion system on the shape of Fe_3O_4 were discussed. Magnetic properties of the as-obtained grass-like Fe_3O_4 samples were also examined.

2. Experimental

Analytical grade $FeCl_3 \cdot 6H_2O$ (99.0%), KOH (85.0%), ethylene glycol (EG, 99.5%), *n*-octanol ($CH_3(CH_2)_7OH$, 99.0%), Triton X-100 (OP), and cyclohexane (C_6H_{12}, 99.5%) were purchased from Xilong Chemical Reagent Factory and were used without further purification.

A typical procedure is as follows: two reverse microemulsions were prepared by adding 0.8 mL of 0.02 M $FeCl_3$ ethylene glycol solution and 0.8 mL of 0.06 M KOH aqueous solution into OP/*n*-octanol/cyclohexane system (according to the mass ratio OP/*n*-octanol/cyclohexane = 2.5/2/8), respectively, which were stirred for 10 min at room temperature when the microemulsion became transparent. Then the two microemulsion solutions were mixed slowly and stirred for another 30 min. The resulting solution was transferred to a 30 mL Teflon-lined stainless-steel autoclave and kept at 190 °C for 10 h. After cooling to the room temperature naturally, black products were harvested by centrifugation, and washed with deionized water and absolute ethanol several times, and dried in vacuum at 50 °C for 4 h. Fig. 1 shows the flowchart of the synthesis process of Fe_3O_4.

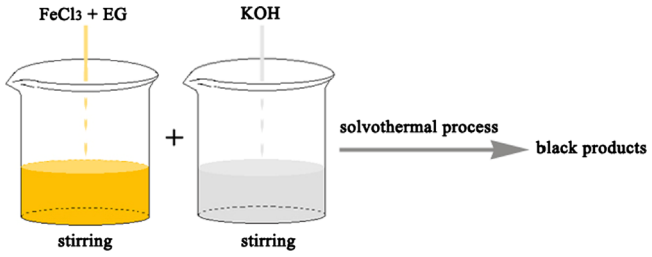

Fig. 1. Flowchart of the typical synthesis process.

Phase identification was done by the powder X-ray diffraction (XRD) using an X-ray diffractometer (the Philips X'Pert) with Cu Kα radiation ($\lambda = 1.5406$ Å). Field emission scanning electron microscopy (FE-SEM) images and energy dispersive X-ray spectroscopy (EDX) analyses were obtained using a Sirion 200 FEG microscope, and the as-synthesized products were dispersed on the Si substrate. The magnetic hysteresis loops were measured by a vibrating sample magnetometer (VSM, Lake Shore 7410).

3. Results and discussion

Fig. 2(a) presents the powder XRD pattern of products obtained at 190 °C for 10 h. All the diffraction peaks can be

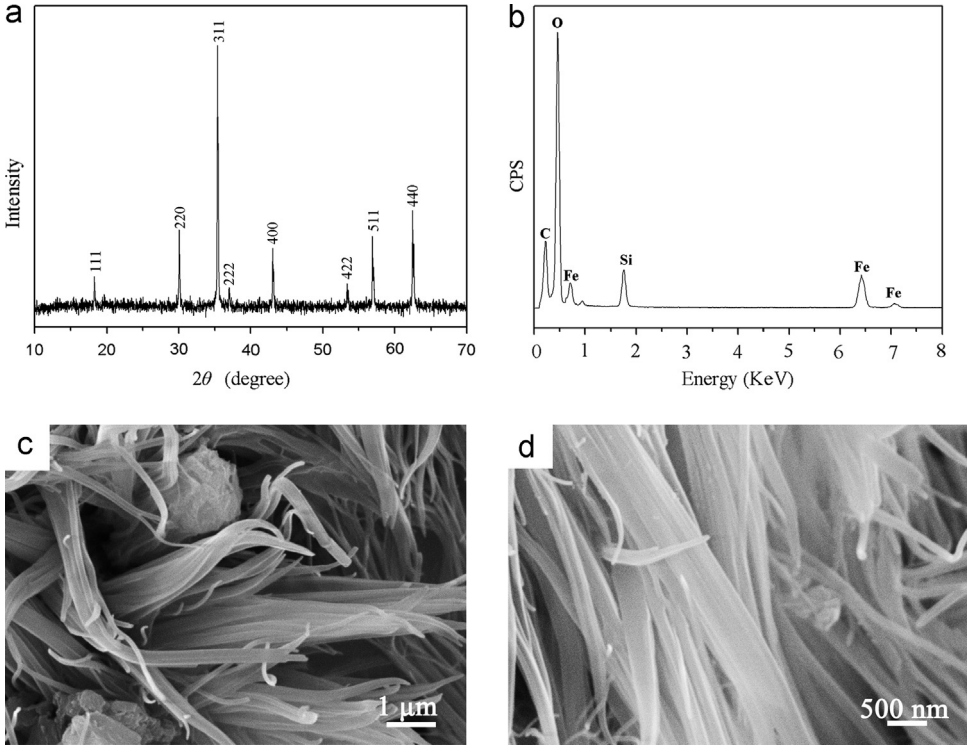

Fig. 2. Structure and morphology of Fe_3O_4 synthesized at 190 °C for 10 h: (a) XRD patterns, (b) EDX data, and (c, d) FE-SEM images.

indexed to cubic-phase Fe_3O_4, and match well with standard cubic Fe_3O_4 (JCPDS no. 65-3107). Elemental analysis (Fig. 2(b)) by EDX confirms the presence of Fe and O elemental signatures. The Si signal comes from the substrate, and C signal could be anticipated from the conducting resin during measurements. Quantitative analysis reports that the atomic ratio of Fe to O is about 3:4, as expected for the stoichiometric composition of Fe_3O_4. Fig. 2(c) and (d) give the representative FE-SEM images of as-formed Fe_3O_4. The results depict that the Fe_3O_4 products are grass-like nanostructures with diameters of 200–300 nm and lengths of tens of micrometers. The surfaces of these well-developed Fe_3O_4 are very smooth and without obvious defects.

It is accepted that many internal or external factors determined the final morphologies of the nanocrystals [28–30]. To better understand the formation of Fe_3O_4 products, several experiments have been carried out under different conditions. First, the effect of reaction temperature on the fabrication of Fe_3O_4 nanostructures was studied. When the temperature was decreased to 140 °C and other synthetic parameters were kept constant, only few irregular short rods were received (Fig. 3(a)). When the temperature was increased to 210 °C, uniform longer nanorods were obtained in large quantity (Fig. 3(b)). It may be because the low temperature increases the viscosity of the microemulsion, slowing down the transfer rate of ions and decreasing the frequency of collisions between ions, therefore, the crystal growth was also restricted. That is, higher reaction temperature would result in higher reaction velocity and then fine-structured Fe_3O_4 [31]. In addition, the experiments revealed that the concentration of KOH is another deciding factor influencing the structure of the final products. When the concentration of KOH was reduced to 0.04 M, small particles with an average diameter of ~30 nm were then assembled into nanochains (Fig. 4(a)). While [KOH] = 0.10 M, irregular massive products instead of grass-like structures were generated (Fig. 4(b)). This phenomenon could be explained by the fact that a high concentration of KOH implies a high chemical potential. High chemical potential is preferable for the growth of one-dimensional nanomaterials [32]. However, higher OH^- ion concentration may disrupt the growth environment of the crystals [33]. Thus, there exists an optimal concentration of KOH for the preparation of grass-like nanostructures. What is more, we noticed that the reverse microemulsion system profoundly impacts the morphology of the

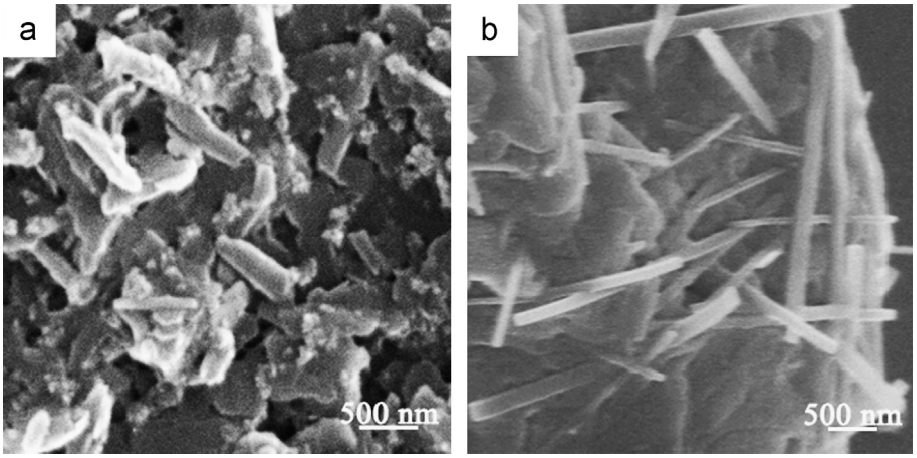

Fig. 3. FE-SEM images of samples prepared in the presence of OP/*n*-octanol/cyclohexane system at varied temperatures for 10 h, with [KOH] = 0.06 M. (a) and (b) are corresponding to 140 and 210 °C, respectively.

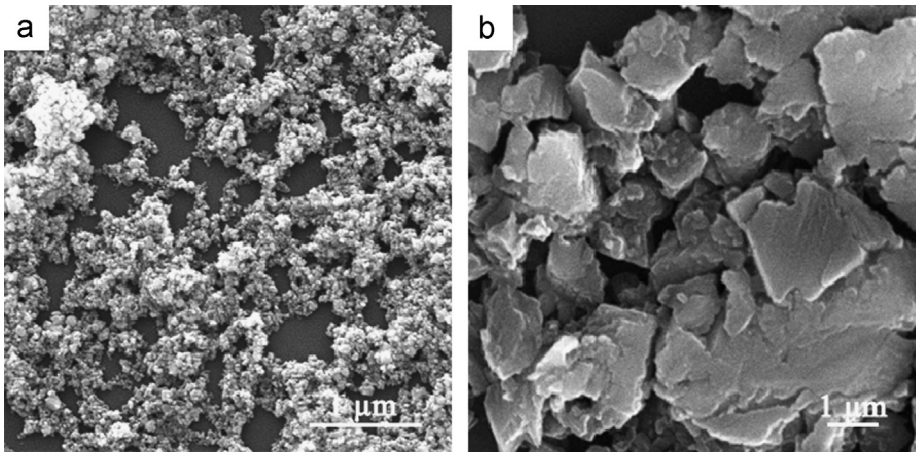

Fig. 4. FE-SEM images of products synthesized in the presence of OP/*n*-octanol/cyclohexane system under different concentrations of KOH: (a) [KOH] = 0.04 M, and (b) [KOH] = 0.10 M. All the samples were prepared at 190 °C for 10 h.

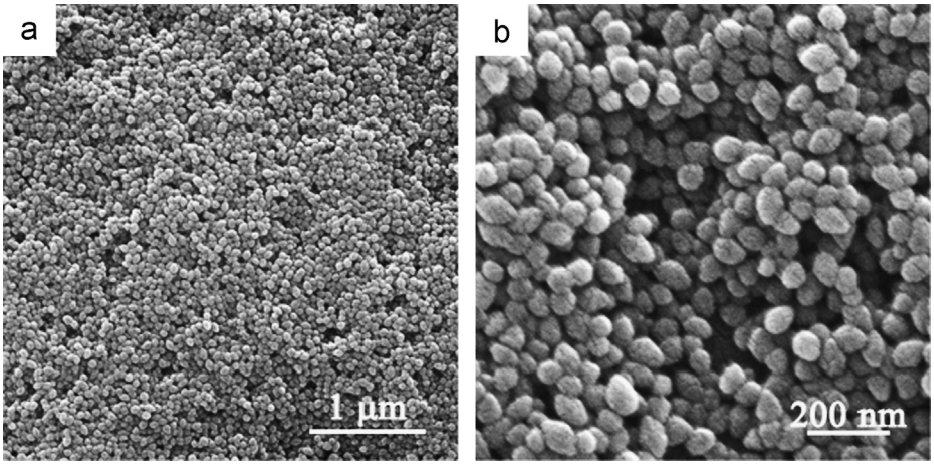

Fig. 5. FE-SEM images of samples fabricated in the absence of OP/*n*-octanol/cyclohexane system at 190 °C for 10 h, with [KOH]=0.06 M.

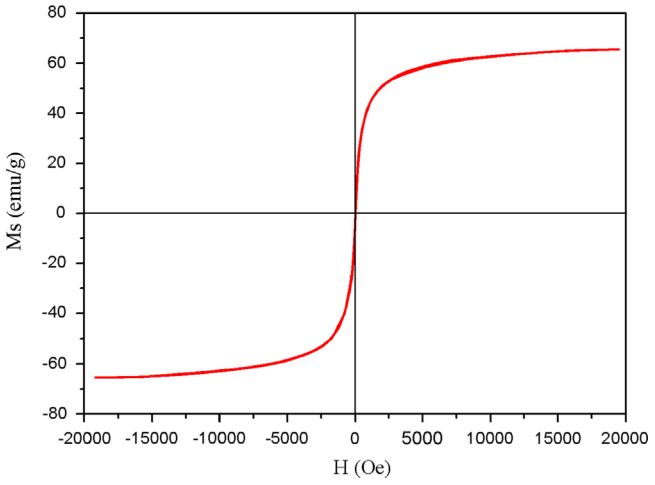

Fig. 6. Room-temperature magnetic hysteresis loops of the as-made Fe_3O_4 grass-like samples.

sample. Without adding OP/*n*-octanol/cyclohexane in the system while keeping other factors fixed, it was found that only high yield homogenous small nanoparticles were developed (Fig. 5(a)). These nanoparticles can be clearly identified to be an ellipsoidal morphology with the average longitudinal axis of 100 nm and horizontal axis of 50 nm (Fig. 5(b)). Previous investigations indicated that the reverse microemulsion system generally served as surfactant-templating in the controlled synthesis of inorganic nanoparticles. Obviously, in this experiment, the OP/*n*-octanol/cyclohexane system was used as a structure-directing template for the preparation of 1D grass-like nanostructure. The above experimental results show that the reaction temperature, the concentration of KOH and the restricting effect of the microemulsion play vital roles in the morphology control, and the grass-like architectures can only be formed and stabilized under certain circumstances. The exact formation mechanism of the grass-like Fe_3O_4 nanostructures needs to be further explored.

It is well known that the magnetic properties of the material are very sensitive to its size, morphology and structure [34]. Magnetic measurements of the grass-like Fe_3O_4 were investigated using VSM with an applied field between 20,000 and 20,000 Oe at room temperature. Fig. 6 lists the *H–M* loop of the as-fabricated grass-like Fe_3O_4, the typical characteristics of superparamagnetic behavior were observed, namely almost immeasurable coercivity and remanence. Saturation magnetization (Ms) was estimated to be 65.5 emu/g. It is smaller than the theoretical value of bulk Fe_3O_4 [35], but higher than that of the belt [36], hollow sphere [37,38], and tube structure [12]. The difference in Ms may be attributed to the size and shape anisotropy [14,39,40]. The in-depth research is still in progress.

4. Conclusions

In summary, we first synthesized the grass-like Fe_3O_4 nanostructures in a reverse microemulsion system under solvothermal treatment. The investigation of the influence factors illustrates that the reaction temperature, the concentration of KOH and the reverse microemulsion system are essential for the morphology control of Fe_3O_4 1D nanostructures. The magnetization measurement elucidates that the as-grown grass-like Fe_3O_4 is superparamagnetic with no hysteresis. These grass-like Fe_3O_4 nanostructures gained from the simple method could have potential applications in different fields. And, this new convenient and sustainable method is expected to be generally applicable for the fabrication of other metal oxides with similar morphologies.

Acknowledgment

The authors acknowledge the financial support from the Fundamental Research Funds for the Central Universities (2012LWA05).

References

[1] Z. Tang, N.A. Kotov, M. Giersig, Spontaneous organization of single CdTe nanoparticles into luminescent nanowires, Science 297 (2002) 237–240.

[2] X. Liang, S. Tan, Z. Tang, N.A. Kotov, Investigation of transversal conductance in semiconductor CdTe nanowires with and without a coaxial silica shell, Langmuir 20 (2004) 1016–1020.
[3] Y.S. Zhao, H.B. Fu, F.Q. Hu, A.D. Peng, W.S. Yang, J.N. Yao, Tunable emission from binary organic one-dimensional nanomaterials: an alternative approach to white-light emission, Advanced Materials 20 (2008) 79–83.
[4] M. Liusar, C. Sanchez, Inorganic and hybrid nanofibrous materials templated with organogelators, Chemistry of Materials 20 (2008) 782–820.
[5] E.V. Shevchenko, D.V. Talapin, H. Schnablegger, A. Kornowski, O. Festin, P. Svedlindh, M. Haase, H. Weller, Study of nucleation and growth in the organometallic synthesis of magnetic alloy nanocrystals: the role of nucleation rate in size control of $CoPt_3$ nanocrystals, Journal of the American Chemical Society 125 (2003) 9090–9101.
[6] J.F. Zhai, M.H. Huang, Y.M. Zhai, S.J. Dong, Magnet-assisted assembly of 1-dimensional hollow PtCo nanomaterials on an electrode surface, Journal of Materials Chemistry 18 (2008) 923–928.
[7] F. Caruso, M. Spasova, A. Susha, M. Giersig, R.A. Caruso, Magnetic nanocomposite particles and hollow spheres constructed by a sequential layering approach, Chemistry of Materials 13 (2001) 109–116.
[8] T. Hyeon, S.S. Lee, J. Park, Y. Chung, H.B. Na, Synthesis of highly crystalline and monodisperse maghemite nanocrystallites without a size-selection process, Journal of the American Chemical Society 123 (2001) 12798–12801.
[9] Y.H. Deng, D.W. Qi, C.H. Deng, X.M. Zhang, D.Y. Zhao, Superparamagnetic high-magnetization microspheres with an Fe_3O_4@SiO_2 core and perpendicularly aligned mesoporous SiO_2 shell for removal of microcystins, Journal of the American Chemical Society 130 (2008) 28–29.
[10] X.W. Liu, Q.Y. Hu, Z. Fang, Q. Wu, Q.B. Xie, Carboxyl enriched monodisperse porous Fe_3O_4 nanoparticles with extraordinary sustained-release property, Langmuir 25 (2009) 7244–7248.
[11] N. Du, Y.F. Xu, H. Zhang, C.X. Zhai, D.R. Yang, Selective synthesis of Fe_2O_3 and Fe_3O_4 nanowires via a single precursor: a general method for metal oxide nanowires, Nanoscale Research Letters 5 (2010) 1295–1300.
[12] W. Wu, X.H. Xiao, S.F. Zhang, J. Zhou, L.X. Fan, F. Ren, C.Z. Jiang, Large-scale and controlled synthesis of iron oxide magnetic short nanotubes: shape evolution, growth mechanism, and magnetic properties, Journal of Physical Chemistry C 114 (2010) 16092–16103.
[13] J. Huang, W.M. Chen, W. Zhao, Y.Q. Li, X.G. Li, C.P. Chen, One-dimensional chainlike arrays of Fe_3O_4 hollow nanospheres synthesized by aging iron nanoparticles in aqueous solution, Journal of Physical Chemistry C 113 (2009) 12067–12071.
[14] K. He, C.Y. Xu, L. Zhen, W.Z. Shao, Hydrothermal synthesis and characterization of single-crystalline Fe_3O_4 nanowires with high aspect ratio and uniformity, Materials Letters 61 (2007) 3159–3162.
[15] S.Y. Chen, J. Feng, X.F. Guo, J.M. Hong, W.P. Ding, One-step wet chemistry for preparation of magnetite nanorods, Materials Letters 59 (2005) 985–988.
[16] M. Chang, N.F. Hsu, C.C. Chung, J.R. Deka, Rapid growth of Fe_3O_4 nanowires with oxide assisted vapor–solid process, Materials Letters 64 (2010) 1077–1080.
[17] T. Muraliganth, A.V. Muruga, A. Manthiram, Facile synthesis of carbon-decorated single- crystalline Fe_3O_4 nanowires and their application as high performance anode in lithium ion batteries, Chemical Communications (2009) 7360–7362.
[18] C.L. Yu, X. Hao, H.T. Jiang, L.L. Wang, Fe_3O_4 nano-whiskers by ultrasonic-aided reduction in concentrated NaOH solution, Particuology 9 (2011) 86–90.
[19] W. Zhang, S.Y. Jia, Q. Wu, J.Y. Ran, S.H. Wu, Y. Liu, Convenient synthesis of anisotropic Fe_3O_4 nanorods by reverse co-precipitation method with magnetic field-assisted, Materials Letters 65 (2011) 1973–1975.
[20] M.P. Pileni, Role of soft colloidal templates in the control of size and shape of inorganic nanocrystals, Nature Materials 2 (2003) 145–150.
[21] M.A. López-Quintela, Synthesis of nanomaterials in microemulsions: formation mechanisms and growth control, Current Opinion in Colloid and Interface Science 8 (2003) 137–144.
[22] C. Tojo, M.C. Blanco, F. Rivadulla, M.A. López-Quintela, Kinetics of the formation of particles in microemulsions, Langmuir 13 (1997) 1970–1977.
[23] M.H. Cao, C.W. Hu, E.B. Wang, The first fluoride one-dimensional nanostructures: microemulsion-mediated hydrothermal synthesis of BaF_2 whiskers, Journal of the American Chemical Society 125 (2003) 11196–11197.
[24] M.H. Cao, X.L. Wu, X.Y. He, C.W. Hu, Microemulsion-mediated solvothermal synthesis of $SrCO_3$ nanostructures, Langmuir 21 (2005) 6093–6096.
[25] Y. Liu, Y. Chu, Surfactant-assisted synthesis of single crystal $BaWO_4$ octahedral microparticles, Materials Chemistry and Physics 92 (2005) 59–63.
[26] Y.F. Li, J.Y. Jiang, Y.J. Ma, G.C. Fan, Z.Y. Huang, C.X. Ban, L.A. Qin, Single-microemulsion-based hydrothermal approach to $In(OH)_3$ and In_2O_3 nanocubes, Chinese Journal of Chemistry 28 (2010) 2188–2192.
[27] J.Y. Jiang, Y.F. Li, S.W. Tan, Z.Y. Huang, Synthesis of zinc oxide nanotetrapods by a novel fast microemulsion-based hydrothermal method, Materials Letters 64 (2010) 2191–2193.
[28] H. Jiang, T. Zhao, C.Z. Li, J. Ma, Hierarchical self-assembly of ultrathin nickel hydroxide nanoflakes for high-performance supercapacitors, Journal of Materials Chemistry 21 (2011) 3818–3823.
[29] Q.Q. Xiong, J.P. Tu, Y. Lu, J. Chen, Y.X. Yu, Y.Q. Qiao, X.L. Wang, C.D. Gu, Synthesis of hierarchical hollow-structured single-crystalline magnetite (Fe_3O_4) microspheres: the highly powerful storage versus lithium as an anode for lithium ion batteries, Journal of Physical Chemistry C 116 (2012) 6495–6502.
[30] H. Jiang, T. Sun, C.Z. Li, J. Ma, Hierarchical porous nanostructures assembled from ultrathin MnO_2 nanoflakes with enhanced supercapacitive performances, Journal of Materials Chemistry 22 (2012) 2751–2756.
[31] S.W. Chao, Y.J. Zhu, Surfactant-free preparation and drug release property of magnetic hollow core/shell hierarchical nanostructures, Journal of Physical Chemistry C 112 (2008) 12149–12156.
[32] Z.A. Peng, X.G. Peng, Mechanisms of the shape evolution of CdSe nanocrystals, Journal of the American Chemical Society 123 (2001) 1389–1395.
[33] R.F. Chen, S.S. Song, Y. Wei, Study on the formation and phase transformation of 1D nanostructured Fe_3O_4 particles under an external magnetic field, Colloids and Surfaces A: Physicochemical and Engineering Aspects 395 (2012) 137–144.
[34] L.J. Zhao, H.J. Zhang, Y. Xing, S.Y. Song, S.Y. Yu, W.D. Shi, X.M. Guo, J.H. Yang, Y.Q. Lei, F. Cao, Morphology-controlled synthesis of magnetites with nanoporous structures and excellent magnetic properties, Chemistry of Materials 20 (2008) 198–204.
[35] D.H. Han, J.P. Wang, H.L. Luo, Crystallite size effect on saturation magnetization of fine ferrimagnetic particles, Journal of Magnetism and Magnetic Materials 136 (1994) 176–182.
[36] L.L. Li, Y. Chu, Y. Liu, D. Wang, Solution-phase synthesis of single-crystalline Fe_3O_4 magnetic nanobelts, Journal of Alloys and Compounds 472 (2009) 271–275.
[37] D.E. Zhang, Z.W. Tong, S.Z. Li, X.B. Zhang, A.L. Ying, Fabrication and characterization of hollow Fe_3O_4 nanospheres in a microemulsion, Materials Letters 62 (2008) 4053–4055.
[38] X.F. Qu, Q.Z. Yao, G.T. Zhou, S.Q. Fu, J.L. Huang, Formation of hollow magnetite microspheres and their evolution into durian-like architectures, Journal of Physical Chemistry C 114 (2010) 8734–8740.
[39] D. Chen, S. Xiong, S.H. Ran, B. Liu, L.M. Wang, G.Z. Shen, One-dimensional iron oxides nanostructures, Science China Physics, Mechanics and Astronomy 54 (2011) 1190–1199.
[40] Z.P. Cheng, X.Z. Chu, J.Z. Yin, H. Zhong, J.M. Xu, Surfactantless synthesis of Fe_3O_4 magnetic nanobelts by a simple hydrothermal process, Materials Letters 75 (2012) 172–174.